



Reprint of: Two-year survey of earthquakes and injection/production wells in the Eagle Ford Shale, Texas, prior to the M_w 4.8 20 October 2011 earthquake ☆,☆☆



Cliff Frohlich ^{a,*}, Michael Brunt ^b

^a Institute for Geophysics, University of Texas at Austin, 10100 Burnet Rd (R2200), Austin, TX 78758, USA

^b Eagle Pass High School, 2020 Second St, Eagle Pass, TX 78852, USA

ARTICLE INFO

Article history:

Accepted 17 July 2013

Editor: P. Shearer

Keywords:

induced earthquakes
injection wells
seismic hazard
energy policy
EarthScope USArray

ABSTRACT

Between November 2009 and September 2011 the EarthScope USArray program deployed ~25 temporary seismograph stations on a 70-km grid in south-central Texas between 27°N–31°N and 96°W–101°W. This area includes the Eagle Ford Shale. For decades this geographic region has produced gas and oil from other strata using conventional methods, but recent developments in hydrofracturing technology has allowed extensive development of natural gas resources from within the Eagle Ford. Our study surveys small-magnitude seismic events and evaluates their correlation with fluid extraction and injection in the Eagle Ford, identifying and locating 62 probable earthquakes, including 58 not reported by the U.S. Geological Survey. The 62 probable earthquakes occur singly or in clusters at 14 foci; of these foci, two were situated near wells injecting recently increased volumes of water; eight were situated near wells extracting recently increased volumes of oil and/or water; and four were not situated near wells reporting significant injection/extraction increases. Thus in this region, while the majority of small earthquakes may be triggered/induced by human activity, they are more often associated with fluid extraction than with injection. We also investigated the M_w 4.8 20 October 2011 Fashing earthquake—the largest historically reported earthquake in south-central Texas—that occurred two weeks after the removal of the temporary USArray stations. A field study indicated that the highest-intensity (MMI VI) region was about 10 km south of 2010–2011 foreshock activity, and that there were no high-volume injection wells within 20 km of the MMI V–VI region or the foreshocks. However, the 20 October 2011 earthquake did coincide with a significant increase in oil/water extraction volumes at wells within the MMI V–VI region, and this was also true for previous earthquakes felt at Fashing in 1973 and 1983. In contrast, our study found significant increases in injection prior to an m_b LG3.6 20 July 1991 earthquake near Falls City, Texas. Thus the Eagle Ford geographic region, with seismic activity associated both with extraction and injection, appears to be more complex than the Barnett Shale of northeast Texas, where a similar survey found possible correlations only with fluid injection.

© 2013 The Authors. Published by Elsevier B.V. All rights reserved.

1. Introduction

While earthquake seismologists have long recognized that fluid injection into the subsurface sometimes triggers earthquakes

(Healy et al., 1968; Hsieh and Bredehoeft, 1981; Nicholson and Wesson, 1990; Suckale, 2009), this phenomenon has gained attention recently (e.g., National Research Council, 2012; Ellsworth, 2013) because earthquakes near injection disposal wells have occurred in several locations where no previous seismicity had been reported historically. These include Dallas–Fort Worth, TX (Frohlich et al., 2011; Janska and Eisner, 2012; Reiter et al., 2012), Cleburne, TX (Howe, 2012), Timpson, TX, and Youngstown, OH. In these cases the injected fluids were generated by shale-gas development projects where wells are hydrofractured to enhance subsurface permeability. The production of gas is accompanied by the flowback of hydrofracture fluids that require disposal, typically accomplished by injecting them elsewhere in designated Class II disposal wells.

DOI of original article: <http://dx.doi.org/10.1016/j.epsl.2013.07.025>.

☆ This is an open-access article distributed under the terms of the Creative Commons Attribution-NonCommercial-No Derivative Works License, which permits non-commercial use, distribution, and reproduction in any medium, provided the original author and source are credited.

☆☆ A publisher's error resulted in this article appearing in the wrong issue. The article is reprinted here for the reader's convenience and for the continuity of the special issue. For citation purposes, please use the original publication details: Earth and Planetary Science Letters 379, pp. 56–63.

* Corresponding author.

E-mail address: cliff@ig.utexas.edu (C. Frohlich).

<http://dx.doi.org/10.1016/j.epsl.2014.06.006>

0012-821X/© 2013 The Authors. Published by Elsevier B.V. All rights reserved.

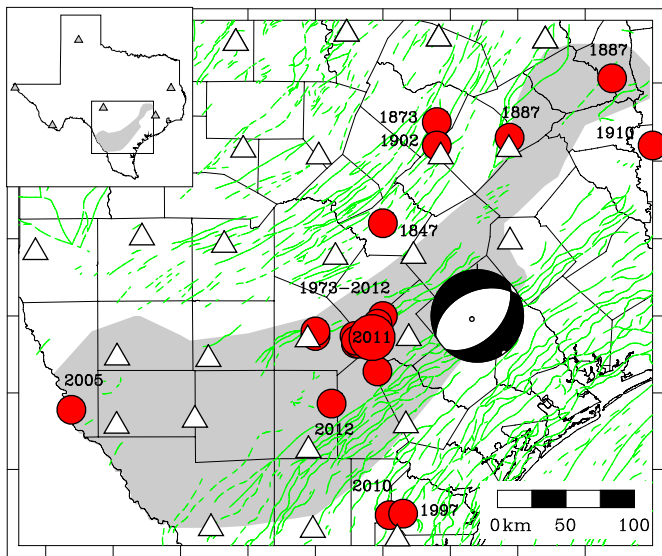


Fig. 1. Map showing extent of Eagle Ford Shale (shaded gray), USArray temporary seismograph stations operating during Nov 2009 to Sept 2011 period (triangles), historical seismicity (red circles; from Frohlich and Davis, 2002; and the NEIC), and mapped faults (green; from Ewing, 1990). Large red circle labeled “2011” is NEIC location for the 20 October 2011 M_w 4.8 earthquake, and beachball at right is focal mechanism determined by the St. Louis group (Herrmann et al., 2011). Other labels indicate year of historical earthquakes. Inset with boundary of Texas shows mapped area and broadband seismograph stations (gray triangles) operating in 2005 prior to passage of the USArray. (For interpretation of the references to color in this figure legend, the reader is referred to the web version of this article.)

This study investigates the relationship between seismicity, fluid injection, and fluid extraction in the Eagle Ford region of south-central Texas (Fig. 1). Gas and oil have been produced extensively from this region since before 1950, mostly from the Edwards formation, a Lower Cretaceous limestone that underlies the Upper Cretaceous Eagle Ford Shale. A series of southwest–northeast fault systems (see Fig. 1), including the Fashing Fault Zone, cuts through much of the Eagle Ford region (Harbor, 2011). Most of these fault systems formed in the proximity of up-dip Triassic/Jurassic salt and result from basinward salt movement (Montgomery, 1990). In some regional fields these faults provide the trap that makes petroleum production viable.

Earthquakes with epicenters within or on the boundaries of producing fields have occurred since a tremor was reported by residents of Fashing, TX, on 25 December 1973 (e.g., Pennington et al., 1986; Olson and Frohlich, 1992; Davis et al., 1995; Frohlich and Davis, 2002). The largest of these earthquakes, with M_w 4.8, occurred on 20 October 2011 near the Fashing Gas Field. Since 2008 the Eagle Ford has been an intense focus of shale-gas development involving extensive hydrofracturing; this raises two questions: (1) Are small earthquakes within the Eagle Ford region associated either with fluid extraction or injection? And (2) Does the evidence indicate the M_w 4.8 20 October 2011 earthquake is of natural origin, triggered by fluid extraction, or triggered by the injection to dispose of flowback brines associated with production and hydrofracturing?

Only a handful of seismograph stations operated in south-central Texas prior to 2009 (Fig. 1); however, the passage of the EarthScope USArray transportable array between 2009 and 2011 provided an unprecedented opportunity to identify and accurately locate earthquakes. The present study will survey seismic activity during this period and evaluate its relationship to both injection and extraction wells. We will compare results from the Eagle Ford region to results from a companion study of the Barnett Shale (Frohlich, 2012). We also present a summary of felt reports for the 20 October 2011 Fashing earthquake.

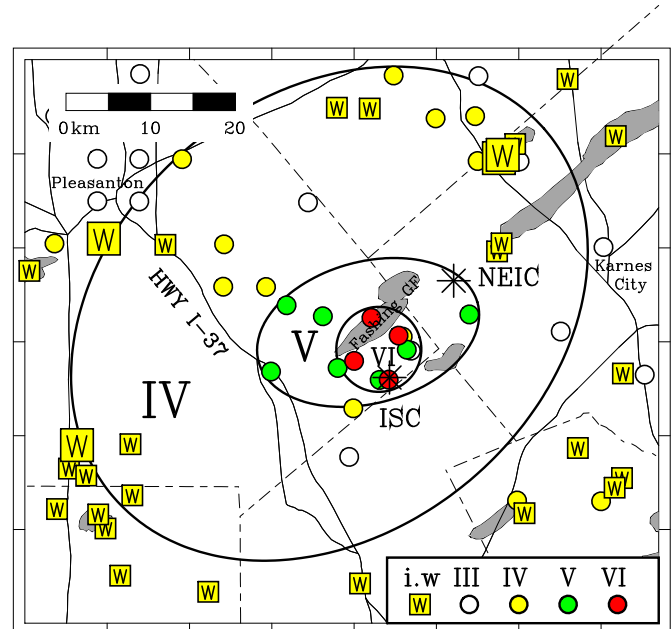


Fig. 2. Map of locations of felt reports (circles) defining the boundaries of regions experiencing modified Mercalli intensity (MMI) IV, V, and VI during the 20 October 2011 earthquake (see also Table S2 and Fig. S2). Yellow squares labeled “W” are injection wells: larger symbols—wells with maximum monthly rates $>100,000$ BWPM ($16,000 \text{ m}^3/\text{mo}$); smaller symbols—wells with maximum monthly rates $>10,000$ BWPM ($1600 \text{ m}^3/\text{mo}$). Stars “*” indicate 20 October 2011 epicenter as reported by the NEIC and ISC. Shaded gray regions are producing oil and gas fields from Galloway et al. (1983) and Kosters et al. (1989). Note that there are no injection wells within ~ 20 km of center of MMI VI area. (For interpretation of the references to color in this figure legend, the reader is referred to the web version of this article.)

The present survey searches for possible correlations between seismicity and extraction/injection rates in the Eagle Ford region. Interpreting the significance of these correlations will require a more thorough analysis of local geology as well as physical modeling of subsurface hydrological/stress. This is the focus of an ongoing companion study for which we hope to enlist industry cooperation concerning the details of subsurface structure.

2. Data and methods

2.1. Felt reports for the 20 October 2011 Fashing earthquake

We gathered felt report information (Fig. S2 and Fig. 2) in two ways. Following the 20 October 2011 earthquake one of the authors (M.B.) spent three days in the epicentral region interviewing residents, concentrating his efforts in the higher-intensity areas. We augmented these data with “Did you feel it?” (DYFI) information provided by the National Earthquake Information Center (NEIC). The DYFI program (Atkinson and Wald, 2007; Wald et al., 2011) is an Internet-based program where individuals can provide unsolicited responses to questions about their experiences and location during an earthquake. The responses are assigned a modified Mercalli intensity (MMI) value; the NEIC routinely presents summary online maps of the MMI distributions. For this study the DYFI data were especially useful for establishing boundaries for the MMI III and MMI IV regions, whereas the in-person interviews constrained the MMI V and MMI VI boundaries that had smaller areal extents but were situated in regions where population was sparse.

2.2. Seismic data and earthquake location

Our procedure for identifying seismic events involved three steps. The first step was to acquire vertical-component seismo-

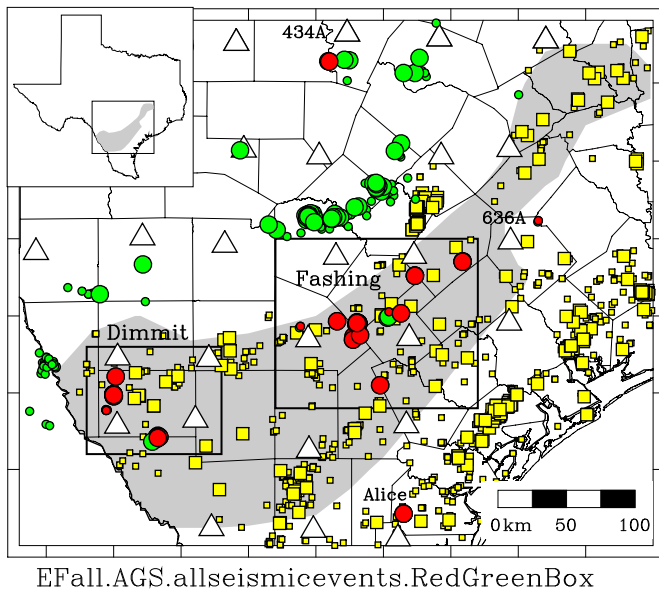


Fig. 3. Map of seismic events (circles) located in this study, injection disposal wells (yellow squares) active October 2006 to November 2009, and USArray temporary stations (triangles). For seismic events, green circles have origin times between 1300 and 2400 hours, corresponding to local daylight work hours 7 AM to 6 PM; red circles occur at other times; larger circles are 'A' quality locations (see text); smaller circles are 'B' quality locations. In several areas events occur only during daylight work hours and are presumably quarry blasts. For injection wells: small symbols—maximum monthly volume >10,000 BWPM (1600 m³/mo); large symbols—maximum monthly volume >100,000 BWPM (16,000 m³/mo). Rectangles labeled 'Dimmit' and 'Fashing' show areas mapped in Figs. 4 and 8; labels near some USArray stations indicate stations mentioned in the text. (For interpretation of the references to color in this figure legend, the reader is referred to the web version of this article.)

grams for the ~25 USArray stations operating in the study area between November 2009 and September 2011. Then, to identify time intervals when locatable seismic events might have occurred, we applied a filter that compared the ratio of the signal short-term average (STA; 4-s interval) and long-term-average (LTA; 1-h interval) of the vertical-component signal. We thus identified 2252 intervals where the STA/LTA ratio exceeded 5.0 during a 30-s interval at four stations.

The second step was to inspect arrivals for these signals, eliminating obvious teleseisms and non-regional seismic events. For this we calculated predicted phase arrival times for phases from selected earthquakes reported by the National Earthquake Information Center (NEIC), the Array Network Facility (ANF) and the Oklahoma seismic network. The third step was to acquire 3-component seismograms for the remaining intervals. For these intervals we picked P- and S-arrival times using Seismic Analysis Code (SAC) software. After some experience had been gained and after making some preliminary locations, we picked only representative events from groups of apparent quarry blasts, i.e., groups of numerous similar seismograms, all occurring during daylight hours, with identical S–P times, large surface waves, and epicenters in or near quarries as identified on GoogleMap.

We located the remaining events using standard iterated least-squares methods and two different flat-layered velocity models modified from regional models described by Mitchell and Landisman (1971), Keller and Shurbet (1975) and Frohlich et al. (2012) (see Table S1). The crustal velocity varies significantly within the study area, and thus we obtained the most accurate locations when we used phase arrivals only from the 4–6 nearest USArray stations surrounding each epicenter. When events occurred in clusters, we reread the P- and S-arrivals within each cluster to ensure that we were picking the same arrival feature for the various

events. The distances separating stations (~70 km) was too large to permit accurate determination of focal depths; thus we fixed focal depths at 5 km for all events. With these procedures we obtained locations for 245 seismic events (Fig. 3).

All earthquake and quarry blast locations in Fig. 3 were determined using arrival picks from at least three nearby stations, including one or more stations with both P and S picks. We graded all locations as 'A' or 'B', with the A-grade given to epicenters determined having an azimuthal gap of 200° or less and residuals of 1.0 s or smaller. We estimate that 'A' quality epicenters are accurate to within about 2 km, and 'B' quality epicenters to within about 4 km. Both are significantly more accurate than NEIC locations for small-magnitude (~M3) Texas earthquakes.

To estimate earthquake magnitudes, we fit the magnitudes M_{NEIC} for events reported by the NEIC to the equation:

$$M_{\text{NEIC}} = a \log_{10}(A_{\text{Max}}) + b/D,$$

where A_{Max} is maximum peak-to-peak signal amplitude as measured in this study and D is event-to-station distance. We then used the coefficients obtained ($a = 0.854$ and $b = -34.5$ km) to calculate M for events not reported by the NEIC, obtaining magnitudes ranging from ~1.5 to 3.0.

2.3. Injection of water; extraction of petroleum and water

Within the Eagle Ford there are thousands of wells drilled for producing oil and natural gas, for injecting water to enhance petroleum production, and for disposing of flowback brines associated routinely with production operations and hydrofracturing. The Texas Railroad Commission (RRC) regulates petroleum wells of all types; they also archive information about permitting history, well locations, depth, and monthly production/injection rates for oil, gas, and water. The RRC database is publicly available online and for individual wells includes monthly injection/production information that is mostly complete for approximately the past three decades. For this study we used RRC data as supplied in more user-friendly form by the company IHS Inc.

3. Results

3.1. Felt reports for the 20 October 2011 Fashing earthquake

The felt area of the Fashing earthquake extended over approximately 11,000 km² (MMI III area), from about 40 km south of Fashing to 90 km north (Table S2 and Fig. S1). The north boundary of the felt area included heavily populated San Antonio; the southern boundary is sparsely populated.

The most intense shaking (MMI VI) occurred within a 64 km² area that extended across the Fashing Gas field (Fig. 2). Here residents reported pictures falling off walls, items falling out of cupboards, and some cracking in masonry and sheet rock. The center of the MMI VI area (Table S2) was at 28.79N 98.17W, 12 km southwest of the epicenter determined by the NEIC (28.865N 98.079W), but only about 3 km from the prime epicenter reported by the International Seismological Center (28.7616N 98.1572W).

3.2. Seismic events: quarry blasts and earthquakes

The majority of events located in this study are probably quarry blasts. Of the 245 seismic events located in this study, 201 (82 per cent) occurred between hours 1300 and 2400; this corresponds to local times 7 AM to 6 PM, i.e., daylight working hours. These daylight events often occurred in clusters; e.g., in Fig. 3 note the cluster north of the 'Fashing' label, the cluster on the U.S.–Mexico border west of the 'Dimmit' label, and the clusters

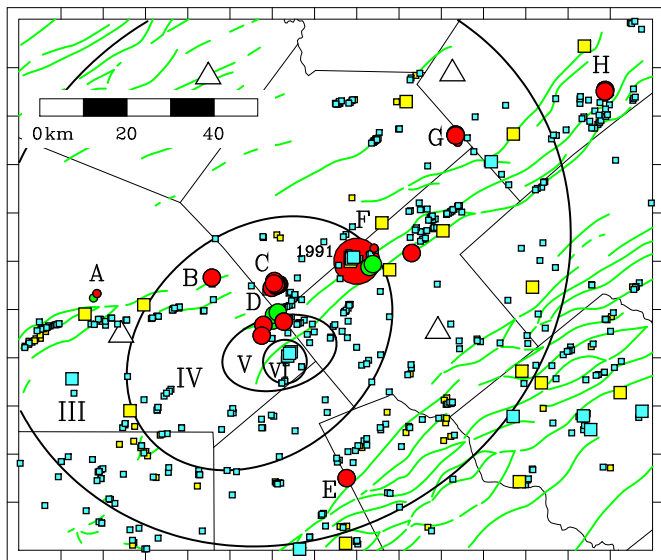


Fig. 4. For Fashing region, map of seismic events (circles, symbols as in Fig. 3), Class II injection wells (yellow squares, symbols as in Fig. 3), wells producing/extracting water (blue squares), USArray stations (triangles), and mapped faults (green; from Ewing, 1990). Labels 'A', 'B', etc. indicate event groups listed in Table S3 and discussed in the text except for the m_{bLG} 3.6 20 July 1991 Falls City earthquake (large red symbol labeled 1991; see text for discussion). Ellipses labeled with Roman numerals III–VI are boundaries of MMI felt areas for the 20 October 2011 M_w 4.8 earthquake (see Figs. 2, 3 and Fig. S1). (For interpretation of the references to color in this figure legend, the reader is referred to the web version of this article.)

south and east of station 434A. Inspection of GoogleMap revealed crushed rock quarries near all of these clusters.

Elsewhere seismic events occurred during both daylight and nighttime hours. We have identified 62 as probable earthquakes (see Table S3). All but five of these occurred in two areas—near Fashing, TX, in Atascosa and Karnes Counties; and in Dimmit County.

3.3. Fashing area: probable earthquakes and injection/production wells

We located 35 probable earthquakes in the Fashing area (Figs. 3 and 4, and Table S3). Since 1982 the International Seismological Centre (ISC) has reported 15 earthquakes within the area mapped in Fig. 4; if we combine these with the probable earthquakes identified in this study, their magnitude–frequency distribution is consistent with a b -value of ~ 1.0 (Fig. 5).

The Fashing events we identified occurred within eight clusters (labeled A–H in Fig. 4), broadly distributed over a ~ 100 -km-long SW–NE trending zone. None of the clusters were situated within the highest-intensity (MMI VI) region of the 20 October 2011 M_w 4.8 earthquake; the closest cluster D was about 10 km northward.

All but three of the Fashing events occurred during the second year of this project, after 20 December 2010—ten months prior to the 20 October 2011 earthquake, and 22 occurred in April or May of 2011, approximately six months prior. These 22 were broadly distributed geographically, including events in clusters A, C, D, G and H. The last event we located occurred on 22 September 2011 (Event #6750, in cluster F). There were no USArray stations in the Fashing area to record the 20 October 2011 earthquake or its aftershocks, as the array moved eastward during the first week of October.

Two of the event clusters, cluster A and cluster F, were situated within 5 km of recently active injection wells (Table 1). Cluster A consists of two earthquakes with magnitude $\sim M_{1.8}$ occurring in May and August of 2011. Since 2000 production of oil and gas has

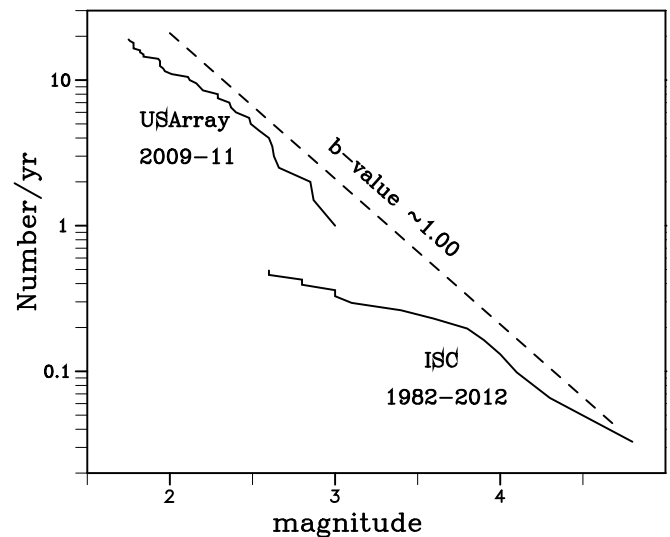


Fig. 5. Magnitude–frequency plots for earthquakes located in Fashing area (Fig. 4). Events labeled 'USArray 2009–11' are as identified in this study (see Table S3); events labeled 'ISC 1982–2012' are as reported by the International Seismological Centre (ISC). Note that a b -value (slope of magnitude–frequency line) of ~ 1.0 is consistent with both event groups.

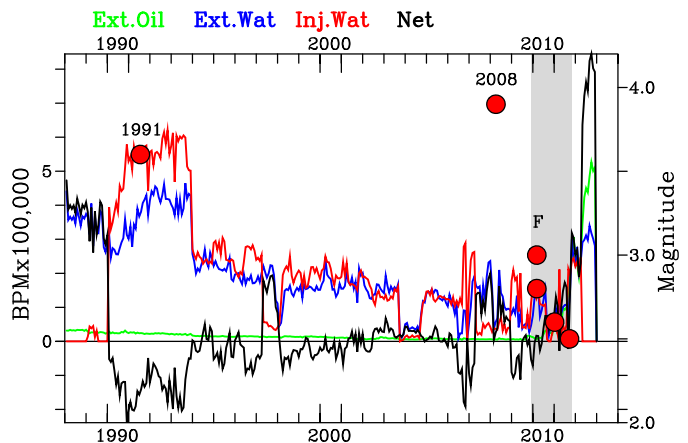


Fig. 6. For wells within 10 km of cluster F ($29^{\circ}N$ $98^{\circ}W$; see Fig. 4), monthly volumes (left axis) for the extraction of oil (green) and water (blue), injection of water (red), and the net (black: oil + water extracted – water injected). Red circles and right axis indicate occurrence and magnitude of earthquakes; gray shaded area indicates time interval when USArray station data was available. Note that m_{bLG} 3.4 23 July 1991 Falls City earthquake followed significant increases in injection beginning in 1990, and the m_b 4.1 7 April 2008 earthquake followed increases in production and injection in late 2006–2007. However, there is no obvious injection/production relationship with cluster F earthquakes. (For interpretation of the references to color in this figure legend, the reader is referred to the web version of this article.)

been negligible within 5 km of cluster A (see Fig. S2), but there are several nearby active injection wells. The closest high-volume injection well [API 14201007611 at ~ 5 km distance] commenced injecting at rates of 10,000–70,000 BWPM (1600 – $11,200$ m^3 /mo) in 2004. Then in March 2011, two months prior to the occurrence of event #6063 on 21 May 2011, injection rates increased to 262,344 BWPM ($42,000$ m^3 /mo), and rates exceeded 190,000 BWPM ($30,400$ m^3 /mo) until November 2011.

The epicenters in cluster F coincide with the maximum-intensity area of the 20 July 1991 m_{bLG} 3.6 Falls City earthquake as determined by Olson and Frohlich (1992). The 1991 earthquake occurred following a large increase in monthly injection rates that began in 1990 (Fig. 6) and exceeded 500,000 BWPM ($80,000$ m^3 /mo) for all but two months between October 1990 and December 1993. There is no obvious relationship to injection

Table 1

Relationship of seismic events/event clusters to injection/extraction. Events/clusters are listed in Table S3 and labeled in Figs. 3, 4, and 8. Injection/extraction increase columns describe monthly sums for all wells within included radius.

Fashing clusters	Number of events	1st event	Injection increase	Wells included radius (km)	Oil/water extraction increase	No increase
A	2	May 2011	Feb 2011: ~200,000 BWPM increase	5		
B	1	Jan 2011		5	Oct–Nov 2010: produced water doubles to 28,000 BWPM	
C	12	Apr 2011		5	Mar 2011: oil + water doubles to ~70,000 BPM	
D	6	Aug 2010		5	Apr 2011: oil + water increases to ~100,000 BPM and more	note increase is after D begins none
E	1	Feb 2011				
F	4	Mar 2010	Jun 2011: ~200,000 BWPM inj. begins	5	Jan–Mar 2010: water increases to 90–100,000 BPM	
G	4	Apr 2011		10	Mar 2011: oil + water increases to ~80,000 BPM	
H	5	May 2011		5	Sep 2010–May 2011: oil + water increases to ~100,000 BPM	
Dimmit clusters	Number of events	1st event	Injection increase	Wells included radius (km)	Oil/water extraction increase	No increase
J	1	Nov 2010	steady injection of ~100,000 BWMP nearby for ~15 yr	5		not an increase
K	7	Jan 2010		5	Nov 2009: sudden water increase to 170,000 BWMP	
L	5	Apr 2010		5	Jan–Apr 2010: sudden increase of water to 10–20,000 BWMP	
M	9	Jun 2011		10	Oct 2010–May 2011: oil + water increases, reaching 290,000 BWMP	
Other events	Number of events	1st event	Injection increase	Wells included radius (km)	Oil/water extraction increase	No increase
434A	2	Sep 2010				none
636A	2	Nov 2010				none
Alice	1	Apr 2010				(complex)

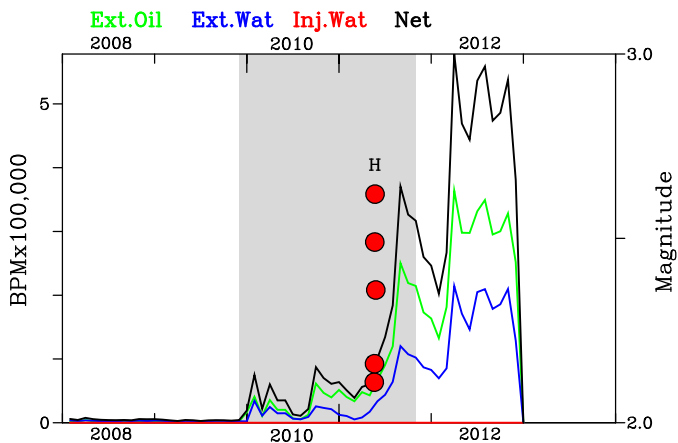


Fig. 7. For wells within 5 km of cluster H (29.353°N 97.413°W; see Fig. 4), monthly volumes (left axis) for the extraction of oil (green) and water (blue), injection of water (red), and the net (black: oil + water extracted – water injected). Red circles and right axis indicate timing and magnitudes of cluster H events; gray shaded area indicates time interval when USArray station data was available. (For interpretation of the references to color in this figure legend, the reader is referred to the web version of this article.)

rates for cluster F epicenters that began occurring in March of 2010 (Fig. S3). However, the extraction of water for wells within 5 km of F events did increase to nearly 100,000 BWPM between January and March of 2010 when the events began.

There are no recently active injection wells nearby clusters B, C, D, E, G and H; however, all but E coincide with increases in production of oil and/or water (Table 1). The B epicenter (Event #5220 in Table S3) occurred two months following a two-month spike in water production at wells within 5 km (Fig. S4). And the G and H activity only began after marked increases in production of oil and water at wells within 10 km (Fig. 7 and Fig. S5).

The C and D clusters are closest geographically to the highest-intensity region of the 20 October 2011 Mw4.8 earthquake. Oil and water production increased sharply near clusters D early in 2011 (Fig. S6) and near cluster C before April 2011 when the activity occurred. Rates of oil + water production remained high throughout most of 2011 and 2012. Although the 20 October 2011 earthquakes occurred following a peak in water production (Fig. S6), the D-cluster events began well before the increase commenced.

If we consider size and time dependence of the clusters A–F, none would be characterized as mainshock–aftershock sequences, with a large earthquake followed by numerous smaller-magnitude events (see Table S3). Instead, when there were several events in a cluster the times were generally swarm-like, with all events having similar magnitudes and occurring within a one- or two-month period (e.g., see clusters C, G, and H).

3.4. Dimmit area: probable earthquakes and injection/production wells

Our investigation identified 22 probable earthquakes (Fig. 8 and Table S3) in Dimmit County, an environment where no earthquakes

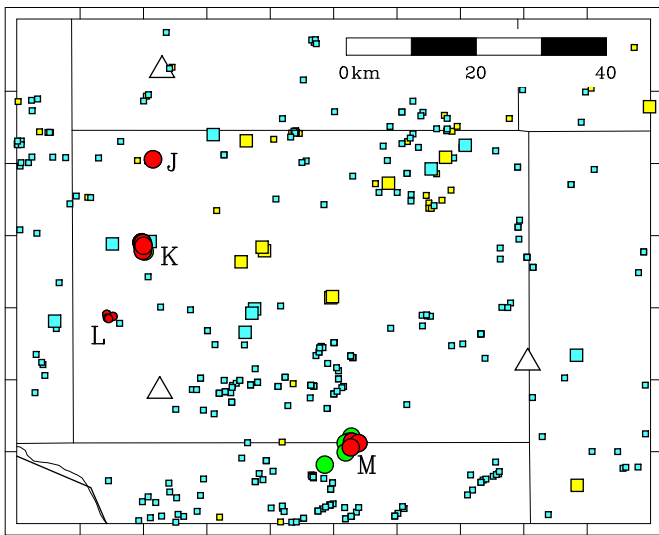


Fig. 8. For Dimmit County and neighboring region (see Fig. 3), map of seismic events (circles; symbols as in Fig. 3), USArray stations (triangles) and wells injecting water (yellow squares) and producing water (blue squares). For wells: small symbols—maximum monthly volume >10,000 BWPM (1600 m³/mo); large symbols—maximum monthly volume >100,000 BWPM (16,000 m³/mo). Labels 'J', 'K', etc. indicate event groups listed in Table S3 and discussed in the text. (For interpretation of the references to color in this figure legend, the reader is referred to the web version of this article.)

had previously been reported. Except for one isolated event (labeled J in Fig. 8; #4728 in Table S3) all occurred in three clusters (K, L and M). The northern cluster K consisted of seven events, and began in January 2010. There were five events in cluster L, all occurring during April 2010, and nine events in cluster M, all in June and July, 2011.

Off these events none except event J occurred near active high-volume injection wells (Table 1). Wells within 5 km of J's location had been injecting at volumes of ~100,000 BWPM since 1996.

In contrast, clusters K, L, and M all are within 5–10 km of wells producing water or oil that reported significant increases in 2009 or 2010. For example, water wells within 5 km of cluster K produced 169,000 BWPM (27,000 m³/mo) in November 2009; the K events began in January 2010 (Fig. S7). Wells within 10 km of M all began producing early in 2010; and for the two months prior to June 2011 when M activity began, their combined extraction of oil and water exceeded 270,000 BPM (Fig. S8). As in the Fashing area, the size and time dependence of Dimmit clusters was more swarm-like than aftershock-like, e.g., all the events in cluster M had magnitudes between 1.9 and 2.7, and all occurred within a three-week period.

3.5. Other probable earthquakes

The remaining probable earthquakes include the $m_{BLG}3.9$ 25 April 2010 earthquake felt widely near Alice, TX (see Fig. 3 and Event #1986 in Table S3) that was the subject of an investigation by Frohlich et al. (2012). Two other isolated events that are probable earthquakes occurred on 18 September 2010 (Events #3906 and #3909 south of station 434A in Fig. 3). Although there are stone quarries that do sometimes generate quarry blasts near this location (a nearby city is named Marble Falls) the seismograms for these two events were distinct, with higher-frequency body waves and smaller surface waves than regional quarry blasts (see Fig. S9). Finally, two probable earthquake events occurred east of station 636A on 2 November 2010 and 9 December 2010 (Events #4484

and #4828 in Table S3). None of these remaining events are near active production or injection wells.

4. Discussion

4.1. Possibly-induced earthquakes and USArray

Like Frohlich's (2012) survey of earthquakes and injection wells in the Barnett Shale of northeast Texas, the present investigation of the Eagle Ford analyzed seismograms collected by the USArray stations to identify small-magnitude seismic events and evaluate their relationship to the extraction/injection of fluids in wells operated by the petroleum industry. Both studies surveyed seismicity in an area undergoing intensive petroleum operations, and evaluated possible relationships between seismicity and human activities. By surveying small-magnitude events, most too small to be reported by the NEIC or felt by local residents, these studies contrast with many investigations of induced/triggered seismicity that are initiated only after an earthquake occurs that is large enough to be felt by local residents and provoke media attention.

Both this study and Frohlich's (2012) survey were possible only because the USArray stations improved event-detection thresholds and increased accuracy of epicenter determination. The USArray program was conceived and funded before there was widespread public concern concerning possible human-caused earthquakes in Texas and elsewhere. Thus these investigations provide apt examples of the potential unanticipated benefits that can follow from large-data gathering programs like USArray, especially when the data are made freely available to all.

From an analysis of USArray data, the present investigation was able to identify 62 small-magnitude events classified as probable earthquakes occurring in/near the Eagle Ford during the November 2009 to September 2011 survey period. Of these events, only four were reported by the NEIC. There were also five earthquakes outside the boundaries of the Eagle Ford (see events near stations 434A and 636A in Fig. 3) including the previously-studied $m_{BLG}3.9$ earthquake occurring in April 2010 near Alice, TX (see Frohlich et al., 2011).

For earthquakes occurring prior to the deployment, and following the removal of the USArray stations, there is often 10 km or more uncertainty in their epicentral location unless felt reports are available to better constrain the epicenter. For example, maximum-intensity foci were established for the $m_{BLG}3.6$ 23 July 1991 and $m_{BLG}4.3$ 9 April 1993 earthquakes near Falls City and Fashing (Olson and Frohlich, 1992; Davis et al., 1995). In contrast, no felt-report survey was undertaken for the $m_b4.1$ 7 April 2008 earthquake and although it was felt in Falls City its exact location is uncertain.

4.2. Relationship of seismicity to injection/extraction

The principal result of this study was that the majority (~90 per cent) of the identified probable earthquakes occurred as single events or clusters at foci near active production or injection wells. Of these foci near active wells, 85 percent occurred near wells where injection or extraction had undergone a significant increase within a year or less prior to the beginning of seismic activity.

However, increases in fluid extraction, rather than injection, occurred prior to the majority of these events and foci (47 of 62 events; 8 of 14 foci). For example, in Dimmit County since 2008 production of water for hydrofracturing and agriculture has increased significantly (Nicot and Scanlon, 2012); 21 of the 22 events (3 of 4 foci) we identified in the Dimmit area (Fig. 8 and Table 1, clusters J–M) appear to be within 5–10 km of such wells. In the Fashing area (Fig. 4 and Table 1, clusters A–F) 28 of the 35 events

(5 of 8 foci) identified are near wells showing increases in oil/water production.

Fluid injection increases at nearby wells did occur prior to seismic events at two foci—foci A in the Fashing region and J in Dimmit County. In addition, our investigation found that the m_{bLG} 3.6 20 July 1991 Falls City earthquake followed an 18-month interval where injection at nearby wells had increased substantially.

These associations between seismic activity and increases in injection/production volumes imply that many of the Eagle Ford earthquakes were triggered/induced. Of course, injection/production activity is nearly ubiquitous throughout much of the Eagle Ford, and in many areas this activity increased markedly in 2010. Thus it is possible that earthquakes of natural origin may occur coincidentally near active wells. However, the observation that most earthquakes identified in this study occurred during the second year of the survey, when regional injection/production rates were generally higher, favors an induced/triggered origin.

The results of this survey indicate the relationship between seismicity and injection/extraction is more complex in the Eagle Ford than in the Barnett. In the Barnett, Frohlich's (2012) two-year survey found that seismic activity was clustered near injection wells, and these were wells having monthly injection rates exceeding 150,000 BWPM (24,000 m³/mo). In the Eagle Ford, our survey finds that seismicity is associated with increases of both injection and extraction, and we were unable to identify a critical monthly rate. In both the Barnett and Eagle Ford there are numerous high-volume production and injection wells with no nearby seismicity.

There are geological and historical differences between the Barnett and the Eagle Ford that may explain the differences in their induced seismicity. In the Eagle Ford region petroleum has been produced by conventional means from various other strata, notably the Edwards formation, for more than 60 yr. The plays are fault bounded and some have been associated with extraction-related earthquakes since the 1970's (Pennington et al., 1986; Davis et al., 1995). In contrast, the induced earthquakes in the Barnett have mostly occurred areas where widespread development took place only within the past ten years (Frohlich, 2012). Thus the differences in Eagle Ford/Barnett induced seismicity may arise partly because human intervention affects a broader variety of geological formations in the Eagle Ford, and partly because features of induced seismicity can change over time scales of decades when injection/extraction is ongoing. This is certainly true for the seismicity associated with injection in Paradox Valley, CO, which has been ongoing for more than 20 yr (Ake et al., 2005).

In both the Eagle Ford and Barnett, as well as many other petroleum-producing regions in the U.S., the sparseness of permanent seismic station coverage is inadequate if we hope to understand why some operations induce earthquakes and others do not. The two-year coverage provided by USArray allows us to identify earthquakes with magnitudes of 2 and smaller and obtain epicenters with uncertainties of ~2 km—often good enough to associate them with particular wells. However, two years is not a sufficiently long interval to obtain unequivocal statistical evidence that particular wells are or are not inducing earthquakes, nor was the station spacing of the USArray network adequate to obtain focal depth information. To better understand the scientific basis of induced earthquakes, for crafting effective policies regulating injection/extraction wells, and for developing effective strategies so that well operators can manage and mitigate the associated hazards, it is desirable to deploy more permanent regional seismic stations, including some densely instrumented networks in targeted areas where induced earthquakes are known to occur.

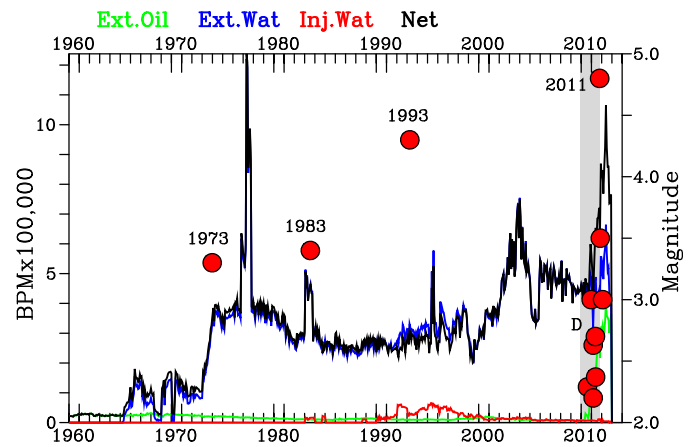


Fig. 9. Fashing earthquakes (red circles, right axis) and monthly volumes (left axis) for the extraction of oil (green) and water (blue), injection of water (red), and net (black: extraction oil + water – injection water) for wells within MMI V region of the 20 October 2011 earthquake (see Fig. 4). Note that earthquakes in 1973, 1983 and 2011 coincide with significant increases in extraction volumes. Gray shaded area indicates time interval when USArray station data was available. (For interpretation of the references to color in this figure legend, the reader is referred to the web version of this article.)

4.3. Was the M_W 4.8 20 October Fashing earthquake induced/triggered?

We find no evidence that fluid injection is responsible for the 20 October 2011 earthquake. Injection is absent or negligible at wells within the MMI-V felt area, and at wells near foreshock clusters D and E. The nearest active high-volume injection wells are about 20 km distant near the site of the 1991 Falls City earthquake—it seems implausible that injection at this distance would induce/trigger the 2011 event.

A comparison of Fashing seismic activity with the 50-yr record of production of petroleum and water in the MMI-V region of the 20 October 2011 earthquake (Fig. 9) suggests there is a relationship between seismic activity and the extraction of fluids (oil + water). The first known Fashing earthquake occurred on 25 December 1973 and followed a marked increase in the production of water at nearby wells that began late in 1971 and first reached 300,000 BWPM (48,000 m³/mo) in November 1973. The m_{bLG} 3.4 earthquake of 23 July 1983 occurred during a nine-month period beginning in January 1983 when water production exceeded 400,000 BWPM (64,000 m³/mo). There is no apparent water-production anomaly associated with the m_{bLG} 4.3 Fashing earthquake of 9 April 1993.

Finally, the M_W 4.8 20 October 2011 earthquake followed increases in the production of oil and water that began in 2010. In fact, it was in October 2011 that the sum of oil + water extraction first exceeded its highest level of the previous three decades (750,000 BPM, or 120,000 m³/mo, in December 2003).

Thus it is plausible that extraction of oil and water induced/triggered the M_W 4.8 20 October 2011 earthquake. This is consistent with the previous studies Fashing-area earthquakes by Pennington et al. (1986) and Davis et al. (1995), who concluded that depressuring of subsurface fluids associated with the extraction of oil and water caused Fashing 1973–1993 earthquakes activity. It is notable that the centers of the maximum-intensity felt areas are virtually identical for the Fashing events of 23 July 1983 (m_{bLG} 3.4), 9 April 1993 (m_{bLG} 4.3), and 20 October 2011 (see Davis et al., 1995; Frohlich and Davis, 2002).

Acknowledgements

We thank David Wald and Vince Quitoriano of the U.S. Geological Survey (USGS) who provided did-you-feel-it (DYFI) information

for constraining the MMI III and MMI IV intensity areas, allowing us to focus our field studies in the higher-intensity areas. This research was partially supported by the USGS, Department of the Interior, under USGS award numbers G12AP20001 and G13AP00023; and by Research Partnership to Secure Energy for America (RPSEA) subcontract #11122-27 through the “Ultra-Deepwater and Unconventional Natural Gas and Other Petroleum Resources” program authorized by the U.S. Energy Policy Act of 2005. RPSEA (www.rpsea.org) is a nonprofit corporation whose mission is to provide a stewardship role in ensuring the focused research, development and deployment of safe and environmentally responsible technology that can effectively deliver hydrocarbons from domestic resources to the citizens of the United States. RPSEA, operating as a consortium of premier U.S. energy research universities, industry, and independent research organizations, manages the program under a contract with the U.S. Department of Energy’s National Energy Technology Laboratory. The views and conclusions contained in this document are those of the authors and should not be interpreted as representing the official policies, either expressed or implied, of the U.S. Government.

Appendix A. Supplementary material

Supplementary tables and figures associated with this article can be found online at <http://dx.doi.org/10.1016/j.epsl.2013.07.025>.

References

- Ake, J., Mahrer, K., O’Connell, D., Block, L., 2005. Deep-injection and closely monitored induced seismicity at Paradox Valley, Colorado. *Bull. Seismol. Soc. Am.* 95, 664–683. <http://dx.doi.org/10.1785/0120040072>.
- Atkinson, G.M., Wald, D.J., 2007. “Did you feel it?” intensity data: A surprisingly good measure of earthquake ground motion. *Seismol. Res. Lett.* 78, 362–368. <http://dx.doi.org/10.1785/gssrl.78.3.362>.
- Davis, S.D., Nyffenegger, P., Frohlich, C., 1995. The 9 April 1993 earthquake in south-central Texas: Was it induced by fluid withdrawal? *Bull. Seismol. Soc. Am.* 85, 1888–1895.
- Ellsworth, W., 2013. Injection-induced earthquakes. *Science* 341, 142–149. <http://dx.doi.org/10.1126/science.1225942>.
- Ewing, T., 1990. Tectonic map of Texas. Univ. Texas Bureau of Economic Geology.
- Frohlich, C., 2012. Two-year survey comparing earthquake activity and injection-well locations in the Barnett Shale, Texas. *Proc. Natl. Acad. Sci.* 109, 13934–13938. <http://dx.doi.org/10.1073/pnas.1207728109>.
- Frohlich, C., Davis, S.D., 2002. *Texas Earthquakes*. Univ. Texas Press, Austin, TX, 275 pp.
- Frohlich, C., Glidewell, J., Brunt, M., 2012. Location and felt reports for the 25 April 2010 mblG3.9 earthquake near Alice, Texas: Was it induced by petroleum production? *Bull. Seismol. Soc. Am.* 102, 457–466. <http://dx.doi.org/10.1785/0120110179>.
- Frohlich, C., Hayward, C., Stump, B., Potter, E., 2011. The Dallas–Fort Worth earthquake sequence: October 2008 through May 2009. *Bull. Seismol. Soc. Am.* 101, 327–340. <http://dx.doi.org/10.1785/0120100131>.
- Galloway, W.E., Ewing, T.E., Garrett, C.M., Tyler, N., Bebout, D.G., 1983. *Atlas of Major Texas Oil Reservoirs*. University of Texas Bureau of Economic Geology, Austin, TX.
- Harbor, R.L., 2011. Facies characterization and stratigraphic architecture of organic-rich mudrocks, upper cretaceous Eagle Ford formation, South Texas. M.S. thesis. University of Texas at Austin. 184 pp.
- Healy, J.H., Ruby, W.W., Griggs, D.T., Raleigh, C.B., 1968. The Denver earthquakes. *Science* 162, 1301–1310.
- Herrmann, R.B., Benz, H., Ammon, C.J., 2011. Monitoring the earthquake source process in North America. *Bull. Seismol. Soc. Am.* 101, 2609–2625. <http://dx.doi.org/10.1785/0120110095>.
- Howe, A.M., 2012. Analysis of Cleburne earthquakes from June 2009 to June 2010. M.S. thesis. Southern Methodist University. 102 pp.
- Hsieh, P.A., Bredehoeft, J.S., 1981. A reservoir analysis of the Denver earthquakes—A case of induced seismicity. *J. Geophys. Res.* 86, 903–920.
- Janska, E., Eisner, L., 2012. Ongoing seismicity in the Dallas–Fort Worth area. *Lead. Edge* 31, 1462–1468.
- Keller, G.R., Shurbet, D.H., 1975. Crustal structure of the Texas Gulf Coastal Plane. *Geol. Soc. Am. Bull.* 86, 807–810.
- Kosters, E.C., Bebout, D.G., Seni, S.J., Garrett, C.M., Brown, L.F., Hamlin, H.S., Dutton, S.P., Ruppel, S.C., Finley, R.J., Tyler, N., 1989. *Atlas of Major Texas Gas Reservoirs*. University of Texas Bureau of Economic Geology, Austin, TX. 161 pp.
- Mitchell, B.J., Landisman, M., 1971. Geophysical measurements in the southern great plains. In: Heacock, J.G. (Ed.), *The Structure and Physical Properties of the Earth’s Crust*. In: AGU Monographs, vol. 14, pp. 77–92.
- Montgomery, S.L., 1990. Horizontal drilling in the Austin Chalk. Part 1, Geology, drilling history and field rules. *Petrol. Front.* 7 (3), 44 pp.
- National Research Council, 2012. *Induced Seismicity Potential in Energy Technologies*. National Academies Press. 225 pp.
- Nicholson, C., Wesson, R.L., 1990. Earthquake hazard associated with deep well injection: A report to the U.S. Environmental Protection Agency. *U.S. Geol. Surv. Bull.* 1951. 74 pp.
- Nicot, J.P., Scanlon, B.R., 2012. Water use for shale-gas production in Texas. *Environ. Sci. Technol.* 46, 3580–3586. <http://dx.doi.org/10.1021/es204602t>.
- Olson, D.R., Frohlich, C., 1992. Felt reports from the 20 July 1991 Falls City earthquake, Karnes County, Texas. *Seismol. Res. Lett.* 63, 5030604.
- Pennington, W.D., Davis, S.D., Carlson, S.M., Dupree, J., Ewing, T.E., 1986. The evolution of seismic barriers and asperities caused by the depressuring of fault planes in oil and gas fields of south Texas. *Bull. Seismol. Soc. Am.* 76, 939–948.
- Reiter, D., Leidig, M., Yoo, S.-H., Mayeda, K., 2012. Source characteristics of seismicity associated with underground wastewater disposal: A case study from the 2008 Dallas–Fort Worth earthquake sequence. *Lead. Edge* 31, 1454–1460.
- Suckale, J., 2009. Induced seismicity in hydrocarbon fields. *Adv. Geophys.* 51, 55–106. [http://dx.doi.org/10.1016/S0065-2687\(09\)05107-3](http://dx.doi.org/10.1016/S0065-2687(09)05107-3).
- Wald, D.J., Quitoriano, V., Worden, B., Hopper, M., Dewey, J.W., 2011. USGS “Did you feel it?” internet-based macroseismic intensity maps. *Ann. Geophys.* 54, 688–707. <http://dx.doi.org/10.4401/ag-5354>.